RESEARCH ARTICLE

Comparative Study of Toxic Effects of Anatase and Rutile Type Nanosized Titanium Dioxide Particles *in vivo* and *in vitro*

Takamasa Numano[1,3], Jiegou Xu[2], Mitsuru Futakuchi[1], Katsumi Fukamachi[1], David B Alexander[2], Fumio Furukawa[3], Jun Kanno[4], Akihiko Hirose[4], Hiroyuki Tsuda[2], Masumi Suzui[1]*

Abstract

Two types of nanosized titanium dioxide, anatase ($anTiO_2$) and rutile ($rnTiO_2$), are widely used in industry, commercial products and biosystems. TiO_2 has been evaluated as a Group 2B carcinogen. Previous reports indicated that $anTiO_2$ is less toxic than $rnTiO_2$, however, under ultraviolet irradiation $anTiO_2$ is more toxic than $rnTiO_2$ *in vitro* because of differences in their crystal structures. In the present study, we compared the *in vivo* and *in vitro* toxic effects induced by $anTiO_2$ and $rnTiO_2$. Female SD rats were treated with 500 μg/ml of $anTiO_2$ or $rnTiO_2$ suspensions by intra-pulmonary spraying 8 times over a two week period. In the lung, treatment with $anTiO_2$ or $rnTiO_2$ increased alveolar macrophage numbers and levels of 8-hydroxydeoxyguanosine (8-OHdG); these increases tended to be lower in the $anTiO_2$ treated group compared to the $rnTiO_2$ treated group. Expression of MIP1α mRNA and protein in lung tissues treated with $anTiO_2$ and $rnTiO_2$ was also significantly up-regulated, with MIP1α mRNA and protein expression significantly lower in the $anTiO_2$ group than in the $rnTiO_2$ group. In cell culture of primary alveolar macrophages (PAM) treated with $anTiO_2$ and $rnTiO_2$, expression of MIP1α mRNA in the PAM and protein in the culture media was significantly higher than in control cultures. Similarly to the *in vivo* results, MIP1α mRNA and protein expression was significantly lower in the $anTiO_2$ treated cultures compared to the $rnTiO_2$ treated cultures. Furthermore, conditioned cell culture media from PAM cultures treated with $anTiO_2$ had less effect on A549 cell proliferation compared to conditioned media from cultures treated with $rnTiO_2$. However, no significant difference was found in the toxicological effects on cell viability of ultra violet irradiated $anTiO_2$ and $rnTiO_2$. In conclusion, our results indicate that $anTiO_2$ is less potent in induction of alveolar macrophage infiltration, 8-OHdG and MIP1α expression in the lung, and growth stimulation of A549 cells *in vitro* than $rnTiO_2$.

Keywords: Nanosized titanium dioxide - anatase - rutile - lung toxicity - MIP1α

Asian Pac J Cancer Prev, **15 (2)**, 929-935

Introduction

There are three mineral forms of natural titanium dioxide particles: rutile, anatase and brookite. Engineered anatase and rutile nanosized titanium dioxide particles ($anTiO_2$ and $rnTiO_2$) are being manufactured in large quantities worldwide and applied in many fields including material industry, electronic industry, commercial products and biosystems. Due to differences in crystal structure, $anTiO_2$ has better photocatalytic activity than $rnTiO_2$ (Kakinoki et al., 2004). Accordingly, $anTiO_2$ is mainly used in paints, such as surface painting of the walls and windows of buildings and vehicles, and photocatalytic systems, while $rnTiO_2$ is preferentially used in cosmetics, sunscreen and food additives.

Large quantity production and widespread application of $nTiO_2$ have given rise to concern about its health and environmental effects. Anatase and rutile type titanium dioxide particles, nanosized and larger, are evaluated as Group 2B carcinogens (possibly carcinogenic to humans) by WHO/International Agency for Research on Cancer (IARC, 2010), based on 2-year animal aerosol inhalation studies (Mohr et al., 2006). Pulmonary exposure to $rnTiO_2$ promotes DHPN-induced lung carcinogenesis in rats, and the promotion effect is possibly associated with $rnTiO_2$ burdened alveolar macrophage derived macrophage inflammatory protein 1 alpha (MIP1α), which acts as a growth factor to stimulate the proliferation of human lung adenocarcinoma cells (A549) *in vitro* (Xu et al., 2010). Dermal application of $anTiO_2$ has been shown to cause significant increases in the level of superoxide dismutase and malondialdehyde in hairless mice (Wu et al., 2009).

Size and photoactivation affect the *in vitro* toxicity of $anTiO_2$ and $rnTiO_2$. $anTiO_2$ (10 and 20 nm) induces

*[1]Department of Molecular Toxicology, Nagoya City University Graduate School of Medical Sciences and Medical School, [2]Laboratory of Nanotoxicology Project, Nagoya City University, Nagoya, [3]DIMS Institute of Medical Science, Aichi, [4]National Institute of Health Sciences, Tokyo, Japan *For correspondence: suzui@med.nagoya-cu.ac.jp*

oxidative DNA damage, lipid peroxidation and micronuclei formation, and increases hydrogen peroxide and nitric oxide production in BEAS-2B cells, a human bronchial epithelial cell line, but anTiO_2 200 nm particles do not (Gurr et al., 2005). In contrast, both nano-sized and 200nm ruTiO_2 are toxic *in vitro* (Gurr et al., 2005; Sayes et al., 2006). On the other hand, under ultraviolet irradiation, anTiO_2 is 100 times more toxic to human dermal fibroblasts and A549 cells than rnTiO_2, and is more potent than rnTiO_2 in the induction of lactate dehydrogenase release, reactive oxygen species production and interleukin 8 secretion (Sayes et al., 2006). Experimental data demonstrating differences in the toxic effects of anTiO_2 and rnTiO_2 *in vivo*, however, are still lacking.

Respiratory exposure to nTiO_2 particles can occur both at the workplace, e.g., in manufacturing and packing sites, and outside the workplace during their use (Maynard et al., 2006; Schulte et al., 2008). In the present study, we delivered anTiO_2 and rnTiO_2 to the rat lung by trans-tracheal intra-pulmonary spraying (TIPS) and compared lung inflammation and several toxicological parameters induced by anTiO_2 and rnTiO_2. The results indicated that obvious lung inflammatory lesions were not observed in the rats, and anTiO_2 or rnTiO_2 particles were phagocytosed by alveolar macrophages. Analysis of alveolar macrophage induction, 8-OHdG level in the lung, and MIP1α expression both *in vivo* in the lung and *in vitro* in PAM indicated that anTiO_2 elicited lower levels of biological responses than rnTiO_2. Long-term toxic effects of anTiO_2 and rnTiO_2 still need to be clarified.

Materials and Methods

Preparation and characterization of nTiO_2 suspension

Nanosized TiO_2 particles (anatase type without coating, primary size 25 nm and rutile type without coating, primary size 20 nm) were provided by Japan Cosmetic Association, Tokyo, Japan. Both anTiO_2 and rnTiO_2 particles were suspended in saline at 500 μg/ml and then autoclaved. The suspensions were sonicated for 20 min shortly before use to prevent aggregate formation.

Characterization of nTiO_2 was conducted as follows: The shapes of nTiO_2 in suspension were imaged by transmission electron microscopy (TEM) and scanning electron microscopy (SEM). Element analysis was performed by a an X-ray microanalyzer (EDAX, Tokyo, Japan), after aliquots of nTiO_2 were loaded onto a carbon sheet. For size distribution analysis, aliquots of the 500 μg/ml nTiO_2 suspension were loaded onto clean glass slides and photographed under a polarized light microscope (Olympus BX51N-31P-O polarized light microscope, Tokyo, Japan), and the photos were then analyzed by an image analyzer system (IPAP, Sumika Technos Corporation, Osaka, Japan). Over 1000 particles of anTiO_2 and rnTiO_2 were measured.

Animals

Female Sprague-Dawley rats (SD rats) were purchased from CLEA Japan Co., Ltd (Tokyo, Japan). The animals were housed in the animal center of Nagoya City University Medical School, maintained on a 12 hour light-dark cycle and received oriental MF basal diet (Oriental Yeast Co., Tokyo, Japan) and water *ad lib*. The research was conducted according to the Guidelines for the Care and Use of Laboratory Animals of Nagoya City University Medical School and the experimental protocol was approved by the Institutional Animal Care and Use Committee (H22M-19).

Trans-tracheal intra-pulmonary spraying (TIPS) protocol

Three groups of 6 female SD rats (Group 1, saline; Group 2, anTiO_2; and Group 3, rnTiO_2) aged 9 weeks were acclimated for 7 days prior to the start of the study. Saline and nTiO_2 suspensions were administered by TIPS to the animals under isoflurane anesthesia: The nozzle of a Microsprayer (series IA-1B Intratracheal Aerosolizer, Penn-century, Philadelphia, PA) connected to a 1 ml syringe was inserted into the trachea through the larynx and a total volume of 0.5 ml suspension was sprayed into the lungs synchronizing with spontaneous inspiration by the animal (Xu et al., 2010). Rats were treated once every the other day over a 2 week period, a total of eight treatments. The total amount of an$TiO_2$and rnTiO_2 administered to Groups 2 and 3 was 2.0 mg per rat. Six hours after the last spraying, the animals were killed and the whole lung was excised and divided into two parts; the left lung was cut into pieces and immediately frozen at -80ºC and used for biochemical analysis, and the right lung was fixed in 4% paraformaldehyde solution in phosphate-buffered saline (PBS) adjusted to pH 7.3 and processed for immunohistochemical, light microscopic and transmission electron microscopic (TEM) examinations.

Light microscopy and transmission electron microscopy

Hematoxylin and eosin (H&E) stained sections were used for pathological observation. The number of alveolar macrophages in H&E lung tissue slides was counted and expressed as number per mm^2.

Slides were observed under light microscopic observation, the corresponding area in the paraffin block was cut out, deparaffinized and embedded in epoxy resin and processed for TEM and titanium element analysis with a JEM-1010 transmission electron microscope (JEOL Co. Ltd, Tokyo, Japan) equipped with an X-ray microanalyzer (EDAX, Tokyo, Japan).

Analysis of 8-hydroxydeoxy guanosine levels

For the analysis of 8-hydroxydeoxyguanosine (8-OHdG) levels, genomic DNA was isolated from a piece of the left lung with a DNA Extractor WB kit (Wako Chemicals Co. Ltd). 8-OHdG levels were determined with an 8-OHdG ELISA Check kit (Japan Institute for Control of Aging, Shizuoka, Japan).

RNA isolation, cDNA synthesis and RT-PCR analysis of gene expression

Pieces of the left lungs (50-100 mg) were thawed, rinsed 3 times with ice cold PBS, and total RNA was isolated using 1 ml Trizol Reagent (Invitrogen, Karlsruhe, Germany). For reverse transcription PCR (RT-PCR) and real-time PCR, first strand cDNA synthesis from 2 mg of total RNA was performed using SuperScript™ III First-Strand Synthesis

System (Invitrogen of Life Technologies, CA) according to the manufacturer's instructions. PCR primers for rat MIP1α were 5'-TTTTGAGACCAGCAGCCTTT -3' (forward) and 5'- CTCAAGCCCCTGCTCTACAC-3' (reverse), and the product size was 191bp. b-actin was used as internal control and the primers were 5'- AGCCATGTACGTAGCCATCC-3' (forward) and 5'-CTCTCAGCTGTGGTGGTGAA-3', and the product size was 228 bp. RT-PCR was conducted using an iCycler (BioRad Life Sciences, CA) as follows: 95°C 20 sec, 60°C 20 sec, 72°C 30sec, 30 cycles for MIP1α; and 95°C 20 sec, 60°C 20 sec, 72°C 30sec, 15 cycles for b-actin. Real-time PCR analysis of MIP1α gene expression was performed with a 7300 Real Time PCR System (Applied Biosystem, CA) using Power SYBR Green PCR Master Mix (Applied Biosystem, CA) according to the manufacturer's instructions. b-actin gene was used as the normalizing reference gene.

Immunohistochemical analysis

Paraffin embedded lung tissues sections were immunostained with polyclonal anti-rat MIP1α (BioVision, Lyon, France). Antigen retrieval was carried out by microwave for 20 min in 10 mmol/L citrate buffer (pH 6.0). Antibody was diluted 1:100 in blocking solution and applied to the slides, and the slides were incubated at 4ºC overnight. Immunohistochemical staining was done by the avidin-biotin complex method (ABC) using the Vectastain Elite ABC system (Vector Laboratories, Burlingame, CA). Biotinylated goat anti-rabbit IgG (Vector Laboratories) was used as a secondary antibody at a dilution of 1:500 for 1 hour and visualized using avidin-conjugated alkaline phosphatase complex (ABC kit, Vector laboratories) and Alkaline Phosphatase Substrate Kit (Vector Laboratories). Sections were lightly counterstained with hematoxylin for microscopic examination.

ELISA for MIP1α in the lung tissues and the supernatants of cell culture

Left lung tissue samples (50-100mg) were thawed, rinsed 3 times with ice cold PBS and homogenized in 1 ml of tissue extraction reagent (PeproTech, London, UK) containing 1% (v/v) Proteinase Inhibitor Cocktail (Sigma-Aldrich, St Louis, MO, USA). The homogenates were clarified by centrifugation at 10,000g, 4ºC for 5 min. The protein content in the supernatants was measured with a BCATM Protein assay kit (Pierce). The levels of MIP1α in the supernatants were measured using rat MIP1α ELISA Development Kit (Cat#: 900-K75, Peprotech, Inc., Rocky Hill, NJ.) according to the manufacturer's instruction, and expressed as pg/mg lung tissue protein. The levels of MIP1α in cell culture supernatants were measured as described above and expressed as pg/ml.

Isolation of PAM and exposure of $nTiO_2$ to PAM cells

Induction and isolation of alveolar macrophages in female SD rats was performed as described previously (Xu et al., 2010). 10^6 primary alveolar macrophages (PAM) were cultured in RPMI1640 containing 2% fetal bovine serum and antibiotics overnight at 37ºC, 5% CO_2. 500 μg/ml of $anTiO_2$ and $rnTiO_2$ suspensions was then added to the cultures to a final concentration of 10 μg/ml and the cells were incubated for another 24 hours. RNA was isolated from the PAM and the level of MIP1α protein in the conditioned culture media was measured by ELISA.

In vitro cell proliferation assay

A549 cells were seeded into 96-well culture plates at 2×10^3 cells per well in 2% fetal bovine serum Dulbecco's modified Eagle's medium (Wako Chemicals Co., Ltd). After overnight incubation, the medium was replaced with the conditioned PAM culture media treated with $anTiO_2$ or $rnTiO_2$, and the cells were incubated for another 72 hours, with or without 20 μg/ml of anti-MIP1α neutralizing antibody (R&D Systems, Minneapolis, MN). The relative cell number of A549 cells was determined using a Cell counting Kit-8 (Dojindo Molecular Technologies, Rockville, MD) according to the manufacturer's instruction.

Cytotoxicity assay in vitro

A549 cells, the primary human lung fibroblast cell line CCD34 (ECACC, Cat. No. 90110514) and PAM were used for cytotoxicity analyses. Cells were seeded in 96 well plates at 5×10^3/well and incubated overnight. The cells were then treated with $anTiO_2$ and $rnTiO_2$ suspensions at final concentrations of 0, 2, 10, or 50 μg/ml and then incubated for another 24 hours. The relative cell number was determined as described above.

Cytotoxicity of $anTiO_2$ and $rnTiO_2$ under ultraviolet B irradiation

A549 cells were used for analysis of $nTiO_2$ cytotoxicity under ultraviolet irradiation. First, we determined an irradiation time that did not affect the cell viability as follows: A549 cells were seeded into 96 well plates at 1×10^3/well in 200 μL Dulbecco's modified Eagle's medium (Wako Chemicals Co., Ltd) containing 10% fetal bovine serum and incubated overnight. The cells were irradiated with ultraviolet B (UVB) for 0, 30 sec, 1 min, 2 min, 5 min and 10 min with a transilluminator (Vilber Lourmat, France). The light intensity was 1000 mW/cm^2, and the emission spectrum was from 270 nm to 330 nm with a peak at 312 nm. The non-irradiated control wells were covered with a sterile aluminium sheet to prevent irradiation. The relative cell number was determined after incubation for 48 hours at 37°C, 5% CO_2.

Next, we observed the effect of $anTiO_2$ and $rnTiO_2$ on cell viability under UVB. A549 cells were seeded into 96 well plate at 1×10^3well in 100 μL culture media and incubated overnight. Then, 100 mL of $anTiO_2$ or $rnTiO_2$ suspensions in DMEM culture medium containing 10% FBS was added into the wells to final concentration of 0, 2, 5 and 10 μg/ml and incubated for 30 min. The cells were irradiated with UVB for 2 min (2 min UVB irradiation did not affect cell viability), and incubated for another 48 hours, before determination of relative cell number.

Statistical and analysis

Statistical significance of the *in vitro* and *in vivo* findings was analyzed using the two-tailed Student's t-test. *In vitro* and *in vivo* data are presented as means±standard

deviations. A value of $p<0.05$ was considered to be significant.

Results

Characterization of $nTiO_2$ particles in suspension

TEM images showed that individual $anTiO_2$ particles were spherical in shape, while individual $rnTiO_2$ particles had a rod-like shape, and both $anTiO_2$ and $rnTiO_2$ formed large aggregates in suspension (Figure. 1A and B). Similarly, SEM observation indicated aggregate formation of both types of $nTiO_2$ particles (Figure. 1C and D). Peaks of titanium (green arrows) and oxygen (blue arrows), which are present in both types of $nTiO_2$ particles, and carbon (white arrows) and nitrogen (red arrow), which are present in the carbon sheets used in the SEM, were observed by elemental scanning (Figure. 1E and F). Peaks of other elements were not detected in either the $rnTiO_2$ or $anTiO_2$ samples. Analyses of particle size showed that the mean and medium diameters were 5.491±2.727 mm and 5.127 mm for $anTiO_2$, and 3.799±2.231 mm and 3.491 mm for $rnTiO_2$ (Figure. 1G), confirming aggregate formation of both types of $nTiO_2$ particles in suspension.

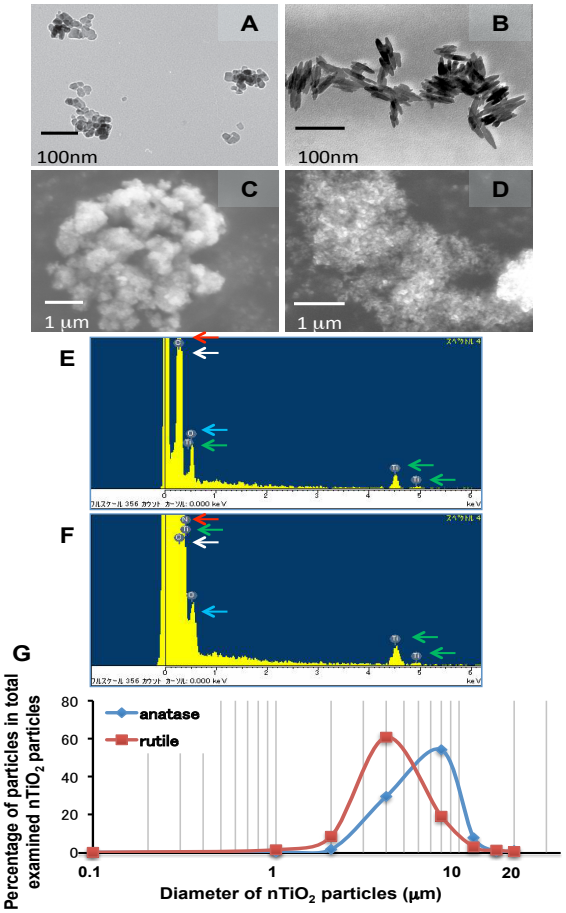

Figure 1. Characterization of $nTiO_2$ Particles in Suspension. A and B: TEM imagines of $anTiO_2$ and $rnTiO_2$ particles in suspension. C and D: SEM images of $anTiO_2$ and $rnTiO_2$ particles. E and F: Element scanning showed peaks of titanium (green arrows), oxygen (blue arrows), carbon (white arrows) and nitrogen (red arrows) in $anTiO_2$ and $rnTiO_2$ particles. G: Size distribution of $anTiO_2$ and $rnTiO_2$ in suspension

Histological observation and 8-OHdG level in the lung tissue

Only a few small lung inflammatory lesions were observed in rats treated with $anTiO_2$ and $rnTiO_2$ (Figure. 2A, B and C). Alveolar macrophage infiltration was found throughout the lung tissue, and most of the alveolar macrophages were seen with phagocytosed $anTiO_2$ particles or $rnTiO_2$ particles (Figure. 2D, E an F). TEM observation demonstrated that both $anTiO_2$ and $rnTiO_2$ were deposited in various sizes in the cytoplasm of the alveolar macrophages (Figure. 2G and H). Neither $anTiO_2$ or $rnTiO_2$ particles were found in other types of cells in the lung tissue. The number of macrophages per mm^2 lung tissue section was 67.1±15.8 (saline), 165.0±34.9 ($anTiO_2$) and 214.2±44.1 ($rnTiO_2$). The numbers of macrophages in the $anTiO_2$ and $rnTiO_2$ treated groups was significantly higher than in the control group ($p<0.001$), and the $anTiO_2$ treated group had lower macrophage infiltration than the $rnTiO_2$ treated group.

The level of 8-OHdG, a parameter of oxidative DNA damage caused by reactive oxygen species (ROS), in the lung tissue in rats treated with $anTiO_2$ and $rnTiO_2$ was 1.96±0.77 and 3.07±1.25 (pg per mg DNA), respectively, and was higher than that of the control (1.44±0.63): The increase in 8-OHdG in the lungs of $rnTiO_2$, but not $anTiO_2$, treated rats was significantly higher than the control

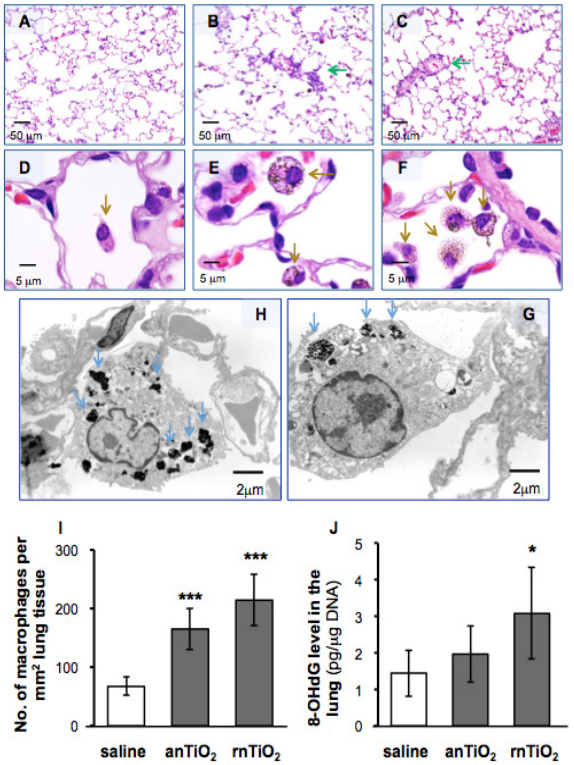

Figure 2. Histological Observation and 8-OHdG Level in the Lung Tissue. A, B and C: Histological imagines of lung tissue treated with saline, $anTiO_2$ and $rnTiO_2$, respectively. Green arrows indicate small inflammatory lesions. D (saline), E ($anTiO_2$) and F ($rnTiO_2$): Higher magnification imagines of alveolar macrophages (brown arrows). $nTiO_2$ particles are clearly observed. G and H: TEM imagines of alveolar macrophages with $anTiO_2$ and $rnTiO_2$ particles in their cytoplasm (blue arrows). I and J: The numbers of alveolar macrophages and 8-OHdG levels in the lung tissue. *, *** represent $p<0.05$ and 0.001, respectively, versus saline

(p<0.05) (Figure. 2J).

MIP1α expression in the lung tissue

RT-PCR suggested an increase in MIP1α mRNA expression in lung tissue treated with $anTiO_2$ or $rnTiO_2$ (Figure. 3A). Real-time PCR analysis indicated that compared with the control group, the increase was 2.79-fold for $anTiO_2$ and 5.35-fold for $rnTiO_2$. MIP1α mRNA expression was also significantly lower in the $anTiO_2$ treated group compared to the $rnTiO_2$ treated group (Figure. 3B). The levels of MIP1α protein in the lung tissue were 32.8±0.31 and 52.7±0.58 pg/mg lung protein in the $anTiO_2$ and $rnTiO_2$ treated groups, both significantly higher than that of the control group (20.8±0.24) (Figure. 3C). Similarly to MIP1α mRNA expression, MIP1α protein expression was significantly lower in the $anTiO_2$ treated group compared to the $rnTiO_2$ treated group.

To find out what cells in the lung accounted for the increased MIP1α protein expression, we examined tissue samples using MIP1α immunohistochemistry. As shown in Figure. 3D, E and F, MIP1α protein was produced by $anTiO_2$ or $anTiO_2$ burdened alveolar macrophages.

Exposure of PAMs to $anTiO_2$ and $rnTiO_2$ and cell proliferation assays in vitro

As in the lung tissue, *in vitro* exposure of PAM to $nTiO_2$ induced expression of MIP1α mRNA (Figure. 4A) and protein (Figure. 4B). Treatment with $anTiO_2$ and $rnTiO_2$ caused 11.96-fold and 15.26-fold increases in the expression of MIP1α mRNA, respectively, in cultured PAM. The level of MIP1α protein in the cell culture medium was 32.8±1.1 pg/mL for $anTiO_2$ and 52.7±1.3 pg/mL for $rnTiO_2$, significantly higher than that of the control

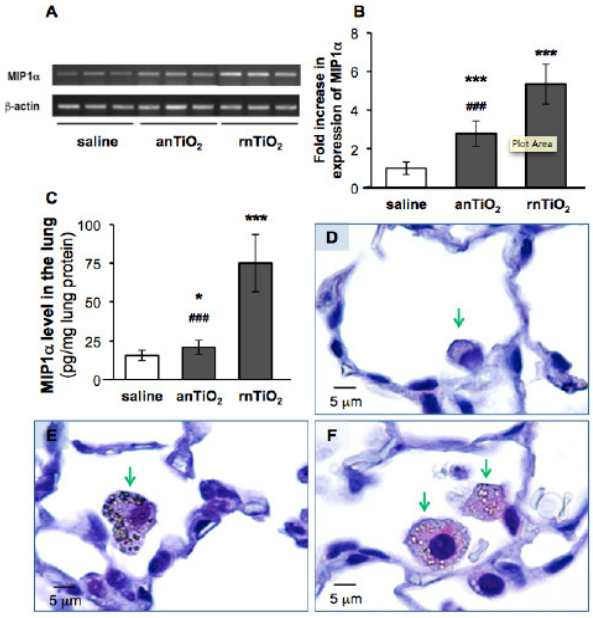

Figure 3. Expression of MIP1α in the Lung Tissue. A, B and C: Analysis of expression of MIP1α mRNA by RT-PCR (A) and real-time PCR (B) and protein by ELISA (C). D, E, and F: Immunohistochemistry shows MIP1α expressed in alveolar macrophages of lung tissue treated with saline (D), $anTiO_2$ (E) and $rnTiO_2$ (F). *, *** represent p<0.05 and 0.001, respectively, versus saline; ### represent p<0.001, versus $rnTiO_2$

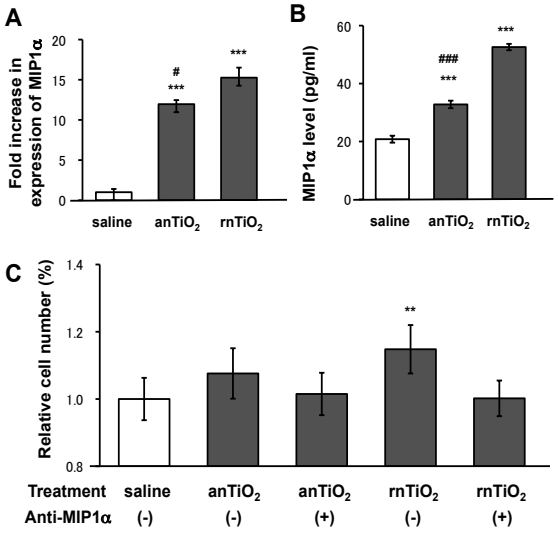

Figure 4. The Effect of $anTiO_2$ and $rnTiO_2$ on PAM Cells. The expression of MIP1α mRNA in cultured PAM (A) and protein in the culture media (B) indicate that treatment with $anTiO_2$ or $rnTiO_2$ increased MIP1α expression in the PAM. Conditioned cell culture media of PAM treated with $rnTiO_2$, but not $anTiO_2$, had a significant effect on proliferation of A549 cells, and this promotion was attenuated by addition of 20 μg/ml MIP1α neutralizing antibody (C). **, ***represent p<0.01 and 0.001, versus saline; #, ###represent p<0.05 and 0.001, versus $rnTiO_2$

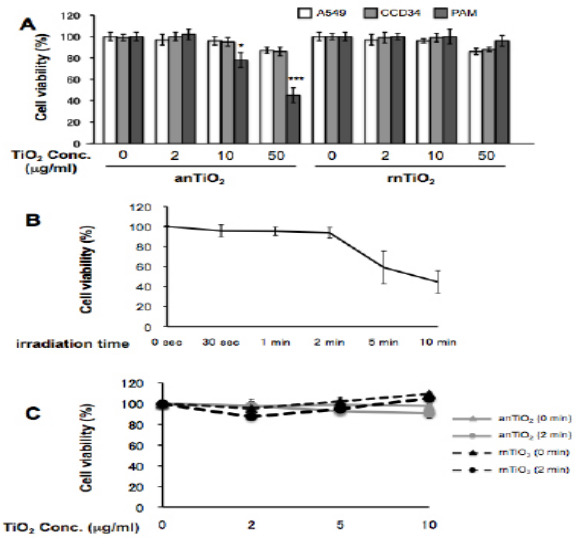

Figure 5. *In vitro* Assays. A: The effect of $anTiO_2$ and $rnTiO_2$ on the viability of A549, CCD34 and PAM cells. B: The effect of UVB irradiation on the viability of A549 cells. C: The effect of $anTiO_2$ and $rnTiO_2$ on the vi ability of A549 under UVB irradiation. *, *** represent p<0.05 and 0.001, versus the vehicle

(20.8±1.2 pg/mL). Both mRNA and protein expression of MIP1α was significantly lower in the $anTiO_2$ treated PAM compared to the $rnTiO_2$ treated cells.

The supernatants of the culture media of PAM treated with $anTiO_2$ showed only a tendency to increase A549 cell proliferation, while those collected from PAM treated with $rnTiO_2$ significantly promoted proliferation of A549 cells (115%) compared to supernatants from the saline treated group (Figure. 4C). The promotion effect of the supernatants of PAM cell cultures treated with $anTiO_2$or

$rnTiO_2$ was attenuated by anti-MIP1α neutralizing antibodies, indicating MIP1α is probably a mediator of the increase in A549 cell proliferation.

In vitro cytotoxicity assays

In vitro cytotoxicity assays indicated that both $anTiO_2$ and $rnTiO_2$ had little effect on the cell viability of A549 and CCD34 cells at a concentration of up to 50 mg/ml. $anTiO_2$ had a cytotoxic effect on the cell viability of PAM at doses of 10 and 50 mg/ml, while $rnTiO_2$ did not impair the cell viability of PAM at any of the examined concentrations (Figure. 5A).

To investigate whether UVB irradiation affected the cytotoxic effects of $anTiO_2$ and $rnTiO_2$ on cell viability, we first determined the exposure times that ultraviolet B irradiation itself did not impair the viability of A549 cells. As shown in Figure. 5B, irradiation for up to 2 min did not have any effect on the viability of A549 cells. With 2 min of UVB irradiation, neither $anTiO_2$ or $rnTiO_2$ at doses of 2, 5 or 10 μg/ml resulted in any decrease in the viability of A549 cells (Figure. 5C).

Discussion

The toxicity of nanoparticles usually includes tiers of biological responses such as induction of ROS and inflammation (Nel et al., 2006). This may contribute to carcinogenic potential (Tsuda et al., 2009). Thus, in the present study, we compared several parameters ofr inflammation and oxidative stress induced by TIPS of $anTiO_2$ and $rnTiO_2$. The results indicated that both $anTiO_2$ and $rnTiO_2$ particles were phagocytosed by alveolar macrophages and did not cause strong lung inflammation. Treatment with $anTiO_2$ and $rnTiO_2$ increased alveolar macrophage infiltration, MIP1α expression and 8-OHdG production: $anTiO_2$ had less effect than $rnTiO_2$.

Phagocytosis by alveolar macrophages is a major defense mechanism for deposition and clearance of inhaled particles (Heppleston, 1984; Rom et al., 1991; Geiser et al., 2008). However, activation of alveolar macrophages is strongly associated with inflammatory reactions and ROS production (Renwick et al., 2001; Bhatt et al., 2002; Wang et al., 2007). Also, MIP1α, secreted from $rnTiO_2$ burden alveolar macrophages, is possibly involved in the promotion of lung carcinogenesis (Xu et al., 2010). Similarly, pleural macrophage recruitment and activation are involved in the pathogenesis of asbestos (Choe et al., 1997). These results indicate two contrasting roles of alveolar macrophages in pathogenesis and host defense.

The toxic effects of nanoparticles are dependent on their size, shape, surface functionality and composition (Albanese et al., 2012). In the present study, we used comparable sizes of $anTiO_2$ and $rnTiO_2$ particles. Both types of $nTiO_2$ had no surface coating and had no obvious difference in elemental composition. Therefore, differences in alveolar macrophage induction, MIP1α expression and 8-OHdG production between $anTiO_2$ and $rnTiO_2$ are likely due to their different crystal structures and shapes. The lower toxicity of $anTiO_2$ compared to $rnTiO_2$ in the absence of UVB irradiation in our study is consistent with a previous *in vitro* study with bulk rutile and anatase TiO_2 (Gurr et al., 2005). In contrast to a previous study (Sayes et al., 2006), in the present study $anTiO_2$ and $rnTiO_2$ did not exhibit different toxicities on the cell viability of A549 cells under ultraviolet irradiation.

It should be noted that both types of $anTiO_2$ and $rnTiO_2$ particles formed aggregates in suspension, and aggregation may alter their bio-reactivity. Whether $anTiO_2$ and $rnTiO_2$ particles have different long-term effects remains to be clarified.

In conclusion, *in vivo* exposure of the rat lung to $anTiO_2$ or $rnTiO_2$ particles increased alveolar macrophage infiltration, MIP1α expression and 8-OHdG production, with $anTiO_2$ eliciting lower levels of biological responses than $rnTiO_2$. Similarly, exposure of primary alveolar macrophages to $rnTiO_2$ *in vitro* resulted the cells producing more MIP1α mRNA and protein than cells exposed to $anTiO_2$. Cytotoxicity assays *in vitro* indicated that both $anTiO_2$ and $rnTiO_2$ had very low cellular toxicity even under UVB irradiation.

Acknowledgements

This work was supported by Health and Labour Sciences Research Grants (Research on Risk of Chemical substance, H19-kagaku-ippan-006 and H22-kagaku-ippan-005). We thank Chisato Ukai and Takako Narita for their excellent secretarial assistance for the work.

References

Albanese A, Tang PS, Chan WC (2012). The effect of nanoparticle size, shape, and surface chemistry on biological systems. *Annu Rev Biomed Eng*, **14**, 1-16.

Bhatt NY, Kelley TW, Khramtsov VV, et al (2002). Macrophage-colony-stimulating factor-induced activation of extracellular-regulated kinase involves phosphatidylinositol 3-kinase and reactive oxygen species in human monocytes. *J Immunol,* **169**, 6427-34.

Choe N, Tanaka S, Xia W, et al (1997). Pleural macrophage recruitment and activation in asbestos-induced pleural injury. *Environ Health Perspect*, *105*, 1257-60.

Geiser M, Casaulta M, Kupferschmid B, et al (2008). The role of macrophages in the clearance of inhaled ultrafine titanium dioxide particles. *Am J Respir Cell Mol Biol*, **38**, 371-6.

Gurr JR, Wang AS, Chen CH, et al (2005). Ultrafine titanium dioxide particles in the absence of photoactivation can induce oxidative damage to human bronchial epithelial cells. *Toxicology,* **213**, 66-73.

Heppleston AG (1984). Pulmonary toxicology of silica, coal and asbestos. *Environ Health Perspect,* **55**, 111-27.

IARC (2010). Carbon black, titanium dioxide, and talc. *IARC Monogr Eval Carcinog Risks Hum*, **93**, 1-413.

Kakinoki K, Yamane K, Teraoka R, et al (2004). Effect of relative humidity on the photocatalytic activity of titanium dioxide and photostability of famotidine. *J Pharm Sci*, **93**, 582-9.

Maynard AD, Aitken RJ, Butz T, et al (2006). Safe handling of nanotechnology. *Nature*, **444**, 267-9.

Mohr U, Ernst H, Roller M, et al (2006). Pulmonary tumor types induced in Wistar rats of the so-called "19-dust study". *Exp Toxicol Pathol*, **58**, 13-20.

Nel A, Xia T, Madler L, et al (2006). Toxic potential of materials at the nanolevel. *Science*, **311**, 622-7.

Renwick LC, Donaldson K, Clouter A (2001). Impairment of alveolar macrophage phagocytosis by ultrafine particles.

Toxicol Appl Pharmacol, **172**, 119-27.

Rom WN, Travis WD, Brody AR (1991). Cellular and molecular basis of the asbestos-related diseases. *Am Rev Respir Dis*, **143**, 408-22.

Sayes CM, Wahi R, Kurian PA, et al (2006). Correlating nanoscale titania structure with toxicity: a cytotoxicity and inflammatory response study with human dermal fibroblasts and human lung epithelial cells. *Toxicol Sci*, **92**, 174-85.

Schulte P, Geraci C, Zumwalde R, et al (2008). Occupational risk management of engineered nanoparticles. *J Occup Environ Hyg*, **5**, 239-49.

Tsuda H, Xu J, Sakai Y, Futakuchi M, Fukamachi K (2009). Toxicology of engineered nanomaterials - A review of carcinogenic potential. *Asian Pac J Cancer Prev*, **10**, 975-980.

Wang H, Li J, Quan X, et al (2007). Formation of hydrogen peroxide and degradation of phenol in synergistic system of pulsed corona discharge combined with TiO_2 photocatalysis. *J Hazard Mater*, **141**, 336-43.

Wu J, Liu W, Xue C, et al (2009). Toxicity and penetration of TiO_2 nanoparticles in hairless mice and porcine skin after subchronic dermal exposure. *Toxicol Lett*, **191**, 1-8.

Xu J, Futakuchi M, Iigo M, et al (2010). Involvement of macrophage inflammatory protein 1alpha (MIP1alpha) in promotion of rat lung and mammary carcinogenic activity of nanoscale titanium dioxide particles administered by intra-pulmonary spraying. *Carcinogenesis*, **31**, 927-35.